Lithuanian Journal of Physics, Vol. **45**, No. 2, pp. 139–147 (2005)

PARAMETERIZATION OF NEW PARTICLE FORMATION AND GROWTH AT THE PREILA STATION

K. Plauškaitė, R. Kazlauskaitė, J. Andriejauskienė, and V. Ulevičius

Environmental Physics and Chemistry Laboratory, Institute of Physics, Savanorių 231, LT-02300 Vilnius, Lithuania
E-mail: ulevicv@ktl.mii.lt

Received 28 February 2005

The aerosol formation and subsequent particle growth in the ambient air have been observed at Preila station located in the coastal/marine environment. Submicron aerosol particle number concentrations and size distributions have been measured using a differential mobility particle sizer (ELAS-5Mc). The studied period covers June, July, and August 1997, June 2000, May 2001, and March, June, July, August, September, and October 2002. In this work, we related the nucleation events to atmospheric circulation and local meteorological parameters. Air mass backward trajectories were used to estimate the prehistory of sampled air. Moreover, trace gas (O_3, NO_x, and SO_2) concentrations were analysed. The observed nucleation mode growth, the source rate of condensable material, and the changes of hygroscopic properties during the nucleation and growth events were analysed. The new particle formation rate, condensation and coagulation sinks were calculated. The growth rates varied between 1.2 and 9.9 nm/h. The formation rate was 0.14 $\mathrm{cm}^{-3}\mathrm{s}^{-1}$. Such a low value of the formation rate could explain why in Preila there are so few event days. The median condensation sink was $1.5{\cdot}10^{-3}$ s^{-1}, and the vapour source rate was $8.06{\cdot}10^{4}$ $\mathrm{cm}^{-3}\mathrm{s}^{-1}$.

Keywords: tropospheric aerosol, nucleation, modelling, air mass backward trajectories, meteorological parameters

PACS: 92.70.Cp, 92.20Bk, 92.60.-e

1. Introduction

Bursts of ultrafine particle concentrations have frequently been observed at several locations in the world in recent years [1]. It is important to know the production mechanisms responsible for these bursts and whether the formed ultrafine particles are able to grow to sizes of radiatively active aerosol and cloud condensation nuclei (CCN) that have a substantial effect on the Earth's radiation budget and climate. The number distributions of atmospheric aerosols are determined by several physicochemical processes, of which the particle formation process involving nucleation and condensational growth to observable sizes is crucial.

In order to understand the nucleation process, identification of the atmospheric perturbations predominantly responsible for it is required. Generally, the probability of new particle formation is connected to the preexisting particle concentration, proper precursors, cloudiness, air mass advection, etc. [2]. Nilsson et al. [3] related the nucleation events to cold air mass advection and explained that events occur more frequently during spring and autumn at larger latitudinal temperature gradients and higher cyclone activity at that time of the year. Nucleation events were also observed in the outflow regions of convective clouds [4] and in regions that had been cleansed by rain [5].

Despite intensive research during several decades, the fundamental mechanism that leads to new particle formation remains uncertain. The binary homogeneous nucleation mechanism of water and sulphuric acid, which has generally been assumed to be the principal mechanism for new particle formation in the atmosphere, is often unable to explain the observed nucleation rates. Alternatively, ternary homogeneous nucleation, also involving ammonia [6], has been suggested as a means of accelerating the nucleation process [7–9].

In this work, we intend to relate the nucleation events to atmospheric circulation and local meteorological parameters. Air mass backward trajectories are used to estimate the prehistory of sampled air. Trace gas (O_3, NO_x, and SO_2) concentrations are analysed together with several meteorological parameters (radiation, temperature, relative humidity, wind speed). The observed nucleation mode growth, the source rate of condensable material, and the changes of hygroscopic properties during the nucleation and growth events are

ISSN 1648-8504

evaluated using equations describing the rate of change of vapour concentration, aerosol particle number concentration, and particle growth.

2. Experimental

The environmental pollution research station in Preila (Lithuania) is located on the Curonian Spit, which separates the Curonian Lagoon and the Baltic Sea. The Curonian Lagoon is a highly eutrophied water body. It is an enclosed shallow (mean depth 3.7 m) bay, connected to the Baltic Sea by the narrow (width 400–600 m) Klaipėda strait. At the Preila station the aerosol particle number concentrations and size distributions in the 10–200 nm size range were measured using differential mobility particle sizer (ELAS-5Mc) developed in the Environmental Physics and Chemistry Laboratory, Institute of Physics, Lithuania. More information can be found in Ulevičius et al. [10]. Meteorological data were provided by the Atmospheric Pollution Research Laboratory, Institute of Physics, Lithuania.

3. Theoretical

3.1. Basic equations

The observed nucleation mode growth, the source rate of condensable material, and the changes of hygroscopic properties during the nucleation and growth events are analysed using three equations describing the rate of change of vapour concentration, aerosol particle number concentration, and particle growth. Considering condensable vapour molecules of species X, the time dependence of vapour concentration C can be expressed (see also [11]) by

$$\frac{\mathrm{d}C}{\mathrm{d}t} = Q - S_{\mathrm{c}} \cdot C \ , \tag{1}$$

where Q is the source rate of the vapour and S_{c} is its condensation sink on the pre-existing aerosol. The time evolution for aerosol number concentration (N) in size i class can be presented by

$$\frac{\mathrm{d}N_i}{\mathrm{d}t} = J_i - S_{\mathrm{coag}} \cdot N_i \ , \tag{2}$$

where J_i is the formation rate of particles and S_{coag} is the coagulation sink for size i particles. The growth rate can be expressed [12] as

$$\frac{\mathrm{d}r}{\mathrm{d}t} = \frac{m_{\mathrm{v}} \beta_m D C}{r \rho} \ . \tag{3}$$

Here r is the particle radius, m_{v} is the molecular mass of condensable vapour, β_m is the transitional correction factor for mass flux, D is the diffusion coefficient, and ρ is the particle density. Equation (3) can be integrated from $r_{_0}$ to r to obtain

$$C = \frac{\rho}{\Delta t \, D \, m_{\mathrm{v}}} \left\{ \frac{r^2 - r_{_0}^2}{2} + \left[\frac{4}{3\alpha} - 0.623 \right] \lambda (r - r_{_0}) \right.$$
$$\left. + 0.623 \lambda^2 \ln \frac{\lambda + r}{\lambda + r_{_0}} \right\} . \tag{4}$$

Here α is the mass accommodation coefficient (i. e., sticking probability) and λ is the mean free path. Directly from measurements of the aerosol size distribution changes and hygroscopicity properties, $\mathrm{d}r/\mathrm{d}t$, S_{c}, S_{coag}, $\mathrm{d}N_{3\,\mathrm{nm}}/\mathrm{d}t$, $N_{\mathrm{nucleation\ mode}}$, and the soluble fraction can be obtained.

Using the above equations and the experimental data, we can also determine J_1 (nucleation rate, or formation rate, for 1 nm particles), where 1 nm is assumed to be the size of a new particle. N_1 is the number concentration of 1 nm particles, N_3 is the number concentration of 3 nm particles. J_3 is the formation rate of 3 nm particles. In order to obtain J_1, we developed a 5-step derivation of J_1.

First, an expression for N_1 is required:

$$\frac{\mathrm{d}N_1}{\mathrm{d}t} = J_1 - K_1 N_1 - J_3 \ , \tag{5}$$

where K_1 is the coagulation sink for 1 nm particles. In practice, it is the coagulation between 1 nm particles and larger particles. Then, assuming a steady-state situation,

$$J_1 = K_1 N_1 + J_3 \ . \tag{6}$$

Second, the link between $K_1 N_1$ and J_3 can be determined referring to the fact that a fraction of N_1 particles will coagulate before they enter the 3 nm size range.

Coagulation of N_1 during the growth from 1 to 3 nm can be obtained from

$$\frac{\mathrm{d}N_{1,3}}{\mathrm{d}t} = -K N_{1,3} \Rightarrow \frac{\mathrm{d}N_{1,3}}{N_{1,3}} = -K \mathrm{d}t$$
$$\Rightarrow N_{1,3} = N_1 \mathrm{e}^{-Kt} \, . \tag{7}$$

Here $N_{1,3}$ corresponds to the concentration of particles growing from 1 to 3 nm, t is the particle growth time, and K is their coagulation sink. Thus, the fraction of

N_1 coagulated during the growth is $1 - \mathrm{e}^{-Kt}$, and the fraction of N_1 contributing to J_3 is e^{-Kt}. Therefore,

$$\frac{K_1 N_1}{J_3} \cong \frac{1 - \mathrm{e}^{-Kt}}{\mathrm{e}^{-Kt}} = \mathrm{e}^{Kt} - 1 \,, \tag{8}$$

and $K_1 N_1 = J_3(\mathrm{e}^{Kt} - 1)$.

Third, combining the above for J_1,

$$J_1 = K_1 N_1 + J_3 = J_3(\mathrm{e}^{Kt} - 1) + J_3 = J_3 \mathrm{e}^{Kt} \,. \tag{9}$$

Fourth, as the equation for N_3 is

$$\frac{\mathrm{d}N_3}{\mathrm{d}t} = J_3 - K_3 N_3 \,, \tag{10}$$

then it follows that

$$J_3 = \frac{\mathrm{d}N_3}{\mathrm{d}t} + K_3 N_3 \,. \tag{11}$$

Finally, J_1 is given by

$$J_1 = J_3 \mathrm{e}^{Kt} = \left(\frac{\mathrm{d}N_3}{\mathrm{d}t} + K_3 N_3 \right) \mathrm{e}^{Kt} \,. \tag{12}$$

The time t in equations above corresponds to the particle growth time from 1 to 3 nm, and K is a typical coagulation sink during the growth, the actual value of which is close to K_1.

In practice, $\mathrm{d}N_3/\mathrm{d}t$ and N_3 are the formation rate of 3 nm particles and the number concentration of nucleation mode particles (larger than 3 nm). Therefore in Eq. (10) there is no condensational transport term that would move particles to larger sizes.

3.2. Condensation sink S_c

The aerosol condensation sink determines how fast the molecules would condense onto pre-existing aerosol and it strongly depends on the shape of the size distribution [13]. As an example, the concentration of sulphuric acid [SA], which is determined by chemical production, nucleation, and condensation, can be expressed by

$$\frac{\mathrm{d}[\mathrm{SA}]}{\mathrm{d}t} = k \cdot [\mathrm{OH}] \cdot [\mathrm{SO_2}] - J \cdot n^* - 4\pi S_\mathrm{c} \cdot D([\mathrm{SA}] - [\mathrm{SA}]_r) \,, \tag{13}$$

where k is the chemical reaction rate constant, n^* is the number of sulphuric acid molecules in the critical cluster. The condensation sink S_c is $4\pi D$, S'_c, and S'_c is integrated over the aerosol size distribution:

$$S'_\mathrm{c} = \int_0^\infty r \beta_M(r)\, n(r)\, \mathrm{d}r = \sum_i \beta_M r_i N_i \,. \tag{14}$$

Here the transitional correction factor β_M can be expressed [14] as

$$\beta_M = \frac{\mathrm{Kn} + 1}{0.377\mathrm{Kn} + 1 + \frac{4}{3}\alpha^{-1}\mathrm{Kn}^2 + \frac{4}{3}\alpha^{-1}\mathrm{Kn}} \,. \tag{15}$$

The Knudsen number $\mathrm{Kn} = \lambda_\mathrm{v}/r$, and the sticking coefficient α is typically assumed to be unity. In the molecular regime where $\mathrm{Kn} \gg 1$ we have $\beta_M \approx 3r/(4\lambda_\mathrm{v})$ and $S_\mathrm{c} \propto r^2$. On the other hand, in the continuum regime where $\mathrm{Kn} \ll 1$ we get $\beta_M = 1$ and $S_\mathrm{c} \propto r$. However, typical tropospheric aerosol also includes the transitional regime and $S_\mathrm{c} \propto r^a$, where $1 < a < 2$.

3.3. Coagulation sink S_coag

The coagulation sink determines how fast the nm-size aerosol particles are removed due to coagulation. The coagulation sink can be determined from

$$S_\mathrm{coag} = \sum_j K_{ij} N_j \,. \tag{16}$$

Here K_{ij} is the coagulation coefficient [15, 16], which in the transitional regime is

$$K_{12} = \frac{K_C^B}{\dfrac{R_{12}}{R_{12} + \sigma_{12}} + \dfrac{4D_{12}}{\overline{c}_{12} R_{12}}} \,, \tag{17}$$

where $K_C^B = 4\pi(R_1 + R_2)(D_1 + D_2)$ is the coagulation coefficient in the continuum regime, $D_i = k_\mathrm{B} T C_\mathrm{C}/(6\pi\mu R_i)$ is the particle diffusion coefficient, and μ is the gas dynamic viscosity.

The Cunningham correction factor is given by $C_\mathrm{C} = 1 + \mathrm{Kn}(\alpha_1 + \alpha_2 \exp(-\alpha_3/\mathrm{Kn}))$, where Kn is calculated for air, and $\alpha_1 = 1.142$, $\alpha_2 = 0.558$, $\alpha_3 = 0.999$ [17].

In the coagulation coefficient, $R_{12} = R_1 + R_2$, $D_{12} = D_1 + D_2$, and $\overline{c}_{12} = \sqrt{\overline{c}_1^2 + \overline{c}_2^2}$ is the mean relative thermal velocity between the particles, $\overline{c}_i = \sqrt{8 k_\mathrm{B} T/(\pi m_i)}$ is the average velocity of particle i with mass m_i, $\sigma_{12} = \sqrt{\varpi_1^2 + \varpi_2^2}$ is the distance at which the two fluxes are matched, $\varpi_i = [(R_{12} + \gamma_i)^3 - (R_{12}^2 + \gamma_i^2)^{3/2}]/(3R_{12}\gamma_i) - R_{12}$, where $\gamma_i = 8D_i/(\pi \overline{c}_i)$ [15].

4. Results

4.1. Air mass trajectories

For the Preila station the series of two day air mass backward trajectories were calculated for June, July,

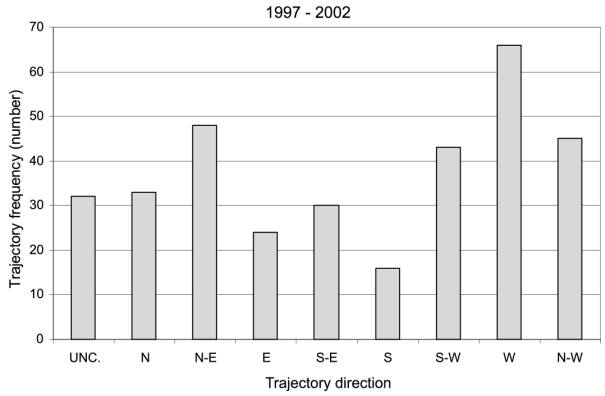

Fig. 1. Frequency of coming air mass calculated using backward trajectories for Preila. The total number of calculated trajectories is 337.

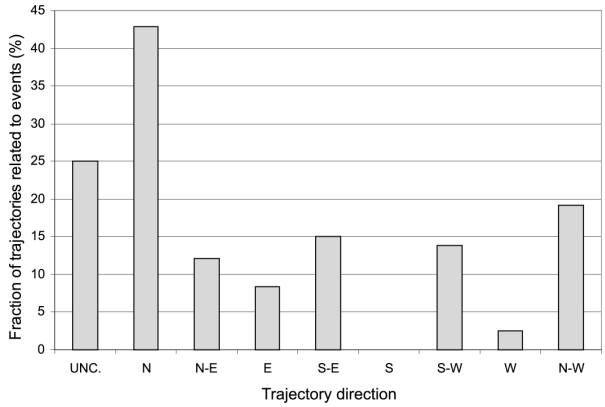

Fig. 2. Fraction of trajectories associated with nucleation events (March, June–October 2002).

and August 1997, June 2000, May 2001, and March, June, July, August, September, and October 2002 using the Hybrid Single-Particle Lagrangian Integrated Trajectories model Version 4 (HY-SPLIT) [18]. The trajectories were plotted on maps and divided into 9 classes corresponding to 8 directions (N, N–W, W, S–W, S, S–E, E, N–E) and those with uncertain origin (coded UNC.).

A classification of the trajectories of air masses coming from different directions is presented in Fig. 1. A clear domination of air masses arriving from the western sector (about 20%) was observed. In summer, a clear domination of air masses originating from Central Europe was observed.

The air mass backward trajectory directions associated with the events are listed in Table 1. Graphically, the same data grouped according to air mass backward trajectories are shown in Fig. 2. In this case all events were classified for the March, June–October 2002 period to get better statistics. For the Preila station, most of the events were accompanied by air masses transported from N and N–W (Figs. 2, 3(c), 4(c)).

4.2. Meteorological parameters

During the measurement period, the highest air temperatures corresponded to air masses originating from south and southeast. The northern air masses obviously caused lower temperatures. The median temperature varied between 13 and 21 °C at daytime. At night, the temperature was approximately 3 °C lower.

The Preila site showed a significantly high radiation. The lowest radiation fluxes corresponded to trajectories from west and southwest, which could be related to higher cloudiness. South was the direction that gave the highest global radiation values in Preila, where the 75th percentile was about 550 $\mathrm{W/m^2}$. June of 2001 was characterized by higher global radiation corresponding to air masses arriving from southeast. A similar situation was for the year 2002, the highest global radiation was when air masses came from east and southeast.

The relative humidity (RH) statistics of the Preila station were evaluated for the entire period of measurement. The Preila station is distinguished for high relative humidity due to marine environment, with a median of relative humidity of 75–95%. The backward trajectory directions and relative humidity do not show any connection in this location.

Due to coastal location, the magnitude of wind speed at the Preila station was high. The medians of wind speed varied between 2.5 and 6.5 $\mathrm{m/s}$. Measurements of wind speed performed in Preila versus the air mass backward trajectories were studied. The highest wind speed was related to the air masses coming from west and northwest.

4.3. Gases

At the Preila station the concentrations of ozone were measured for the entire period. Slightly higher concentrations of ozone were associated with S–E, S, and N–W trajectory directions in 1997. In June 2000 the concentrations at the Preila station were the highest for the whole measurement period for all the directions considered, except N, N–E, and E, as no data for these directions were recorded. The median for this period was between 110 and 130 $\mu\mathrm{g/m^3}$. May 2001 and all the periods in 2002 showed the same trend as in 1997, with similar concentrations and a small difference caused by the air masses coming from southern directions.

The year 1997 was characterized by significantly higher concentrations of NO_x, when a clear southward

Table 1. Calculated characteristics of nucleation events in Preila.

Date	Growth rate, nm/h	J, $\mathrm{cm^{-3}s^{-1}}$	S_c, $\mathrm{s^{-1}}$	Q, $\mathrm{cm^{-3}s^{-1}}$	S_{coag} (1 nm), $\mathrm{s^{-1}}$	S_{coag} (2 nm), $\mathrm{s^{-1}}$	S_{coag} (3 nm), $\mathrm{s^{-1}}$	Trajectory direction
1997.06.05	2.2	0.11	$2.00\cdot10^{-3}$	$6.03\cdot10^{4}$	$1.10\cdot10^{-3}$	$4.00\cdot10^{-4}$	$2.00\cdot10^{-4}$	Northwest
1997.06.11	3.4	0.33	$3.90\cdot10^{-3}$	$1.82\cdot10^{5}$	$5.55\cdot10^{-4}$	$1.77\cdot10^{-4}$	$9.02\cdot10^{-5}$	West
1997.06.21	3.6	0.75	$1.70\cdot10^{-3}$	$8.38\cdot10^{4}$	$1.20\cdot10^{-3}$	$4.00\cdot10^{-4}$	$2.00\cdot10^{-4}$	Southeast
1997.06.25	1.2	0.03	$5.64\cdot10^{-4}$	$9.27\cdot10^{3}$	$3.70\cdot10^{-4}$	$1.20\cdot10^{-4}$	$6.17\cdot10^{-5}$	Uncertain
1997.07.01	5.0	0.22	$9.70\cdot10^{-3}$	$6.64\cdot10^{5}$	$6.90\cdot10^{-3}$	$2.20\cdot10^{-3}$	$1.10\cdot10^{-3}$	Southeast
1997.07.02	6.8	1.91	$1.64\cdot10^{-2}$	$1.53\cdot10^{6}$	$1.00\cdot10^{-2}$	$3.20\cdot10^{-3}$	$1.70\cdot10^{-3}$	Uncertain
1997.07.03	5.2	1.27	$1.66\cdot10^{-2}$	$1.18\cdot10^{6}$	$1.15\cdot10^{-2}$	$3.70\cdot10^{-3}$	$1.90\cdot10^{-3}$	West
1997.07.06	4.6	0.14	$1.09\cdot10^{-2}$	$6.87\cdot10^{5}$	$8.70\cdot10^{-3}$	$2.80\cdot10^{-3}$	$1.40\cdot10^{-3}$	Uncertain
1997.07.09	4.5	0.49	$1.10\cdot10^{-2}$	$6.78\cdot10^{5}$	$5.60\cdot10^{-3}$	$1.80\cdot10^{-3}$	$9.00\cdot10^{-4}$	North
1997.07.11	3.7	0.15	$1.00\cdot10^{-3}$	$5.07\cdot10^{4}$	$5.91\cdot10^{-4}$	$1.97\cdot10^{-4}$	$1.04\cdot10^{-4}$	North
1997.07.18	2.8	0.02	$1.40\cdot10^{-3}$	$5.37\cdot10^{4}$	$6.90\cdot10^{-4}$	$2.23\cdot10^{-4}$	$1.15\cdot10^{-4}$	East
1997.07.20	3.9	0.11	$1.30\cdot10^{-3}$	$6.95\cdot10^{4}$	$7.28\cdot10^{-4}$	$2.33\cdot10^{-4}$	$1.19\cdot10^{-4}$	East
1997.07.22	4.4	0.24	$2.10\cdot10^{-3}$	$1.27\cdot10^{5}$	$1.30\cdot10^{-3}$	$4.00\cdot10^{-4}$	$2.00\cdot10^{-4}$	Northeast
1997.07.24	3.0	0.10	$1.40\cdot10^{-3}$	$5.75\cdot10^{4}$	$7.99\cdot10^{-4}$	$2.60\cdot10^{-4}$	$1.34\cdot10^{-4}$	Uncertain
1997.08.07	2.2	0.10	$1.20\cdot10^{-3}$	$3.62\cdot10^{4}$	$7.47\cdot10^{-4}$	$2.41\cdot10^{-4}$	$1.24\cdot10^{-4}$	Northeast
2000.06.10	3.5	0.08	$1.30\cdot10^{-3}$	$6.23\cdot10^{4}$	$8.75\cdot10^{-4}$	$2.82\cdot10^{-4}$	$1.45\cdot10^{-4}$	West
2000.06.11	3.5	0.25	$1.00\cdot10^{-3}$	$4.80\cdot10^{4}$	$7.80\cdot10^{-4}$	$2.54\cdot10^{-4}$	$1.31\cdot10^{-4}$	Southeast
2000.06.19	5.3	0.35	$1.40\cdot10^{-3}$	$1.02\cdot10^{5}$	$8.91\cdot10^{-4}$	$3.00\cdot10^{-4}$	$1.59\cdot10^{-4}$	Northwest
2001.05.15	9.9	0.55	$8.90\cdot10^{-3}$	$1.21\cdot10^{6}$	$5.20\cdot10^{-3}$	$1.60\cdot10^{-3}$	$8.00\cdot10^{-4}$	Southwest
2002.03.11	1.9	1.09	$8.78\cdot10^{-4}$	$2.29\cdot10^{4}$	$5.15\cdot10^{-4}$	$1.68\cdot10^{-4}$	$8.72\cdot10^{-5}$	Southwest
2002.03.12	1.5	0.15	$1.90\cdot10^{-3}$	$3.90\cdot10^{4}$	$9.59\cdot10^{-4}$	$3.08\cdot10^{-4}$	$1.57\cdot10^{-4}$	Southwest
2002.03.14	4.0	4.97	$7.70\cdot10^{-2}$	$4.22\cdot10^{6}$	$4.50\cdot10^{-2}$	$1.45\cdot10^{-2}$	$7.50\cdot10^{-3}$	North
2002.03.15	1.7	3.60	$5.10\cdot10^{-3}$	$1.19\cdot10^{5}$	$6.60\cdot10^{-3}$	$2.10\cdot10^{-3}$	$1.10\cdot10^{-3}$	Northwest
2002.03.21	3.8	0.14	$2.80\cdot10^{-3}$	$1.46\cdot10^{5}$	$1.50\cdot10^{-3}$	$5.00\cdot10^{-4}$	$3.00\cdot10^{-4}$	Northwest
2002.06.19	6.2	0.01	$7.13\cdot10^{-4}$	$6.06\cdot10^{4}$	$3.42\cdot10^{-4}$	$1.10\cdot10^{-4}$	$5.61\cdot10^{-5}$	Southwest
2002.07.04	8.3	0.06	$1.27\cdot10^{-4}$	$1.44\cdot10^{4}$	$7.85\cdot10^{-5}$	$2.54\cdot10^{-5}$	$1.31\cdot10^{-5}$	Southwest
2002.07.05	7.0	0.32	$4.31\cdot10^{-4}$	$4.13\cdot10^{4}$	$1.71\cdot10^{-4}$	$5.65\cdot10^{-5}$	$2.96\cdot10^{-5}$	West
2002.08.16	4.1	0.03	$2.50\cdot10^{-3}$	$1.40\cdot10^{5}$	$1.60\cdot10^{-3}$	$5.00\cdot10^{-4}$	$3.00\cdot10^{-4}$	North
2002.08.25	5.0	0.08	$2.40\cdot10^{-3}$	$1.64\cdot10^{5}$	$1.30\cdot10^{-3}$	$4.00\cdot10^{-4}$	$2.00\cdot10^{-4}$	East
2002.08.26	2.8	0.11	$2.50\cdot10^{-3}$	$9.59\cdot10^{4}$	$3.00\cdot10^{-3}$	$9.00\cdot10^{-4}$	$5.00\cdot10^{-4}$	Southeast
2002.08.27	2.7	0.08	$2.40\cdot10^{-3}$	$8.88\cdot10^{4}$	$1.50\cdot10^{-3}$	$5.00\cdot10^{-4}$	$2.00\cdot10^{-4}$	Southeast
2002.08.28	4.0	0.51	$3.40\cdot10^{-3}$	$1.86\cdot10^{5}$	$2.00\cdot10^{-3}$	$6.00\cdot10^{-4}$	$3.00\cdot10^{-4}$	Southeast
2002.09.01	5.0	0.03	$6.64\cdot10^{-4}$	$4.55\cdot10^{4}$	$2.79\cdot10^{-4}$	$8.95\cdot10^{-5}$	$4.58\cdot10^{-5}$	Northwest
2002.09.14	3.9	0.01	$5.59\cdot10^{-4}$	$2.99\cdot10^{4}$	$2.79\cdot10^{-4}$	$9.12\cdot10^{-5}$	$4.73\cdot10^{-5}$	Northwest
2002.09.15	3.0	0.05	$4.51\cdot10^{-4}$	$1.85\cdot10^{4}$	$4.89\cdot10^{-4}$	$1.63\cdot10^{-4}$	$8.53\cdot10^{-5}$	North
2002.09.16	2.7	0.06	$2.31\cdot10^{-4}$	$8.56\cdot10^{3}$	$1.06\cdot10^{-4}$	$3.53\cdot10^{-5}$	$1.85\cdot10^{-5}$	North
2002.09.19	6.5	0.09	$3.60\cdot10^{-4}$	$3.21\cdot10^{4}$	$1.92\cdot10^{-4}$	$6.48\cdot10^{-5}$	$3.44\cdot10^{-5}$	North
2002.09.20	5.3	0.06	$1.50\cdot10^{-3}$	$1.09\cdot10^{5}$	$6.93\cdot10^{-4}$	$2.28\cdot10^{-4}$	$1.19\cdot10^{-4}$	Northwest
2002.09.21	4.1	0.04	$1.20\cdot10^{-3}$	$6.74\cdot10^{4}$	$1.00\cdot10^{-3}$	$3.00\cdot10^{-4}$	$2.00\cdot10^{-4}$	Uncertain
2002.09.22	4.2	0.04	$1.40\cdot10^{-3}$	$8.06\cdot10^{4}$	$1.00\cdot10^{-3}$	$3.00\cdot10^{-4}$	$2.00\cdot10^{-4}$	Northeast
2002.09.23	3.5	0.09	$5.42\cdot10^{-4}$	$2.60\cdot10^{4}$	$2.79\cdot10^{-4}$	$9.11\cdot10^{-5}$	$4.72\cdot10^{-5}$	North
2002.09.24	1.5	0.53	$9.02\cdot10^{-4}$	$1.85\cdot10^{4}$	$7.77\cdot10^{-4}$	$2.56\cdot10^{-4}$	$1.33\cdot10^{-4}$	Northwest
2002.09.27	3.9	0.53	$5.00\cdot10^{-3}$	$2.67\cdot10^{5}$	$2.10\cdot10^{-3}$	$7.00\cdot10^{-4}$	$4.00\cdot10^{-4}$	Northeast
2002.10.19	5.4	0.70	$2.50\cdot10^{-3}$	$1.85\cdot10^{5}$	$9.92\cdot10^{-4}$	$3.26\cdot10^{-4}$	$1.70\cdot10^{-4}$	Northeast
2002.10.20	2.3	2.17	$1.11\cdot10^{-2}$	$3.50\cdot10^{5}$	$1.50\cdot10^{-3}$	$5.00\cdot10^{-4}$	$2.00\cdot10^{-4}$	North
Median	3.9	0.14	$1.50\cdot10^{-3}$	$8.06\cdot10^{4}$	$9.59\cdot10^{-4}$	$3.00\cdot10^{-4}$	$1.59\cdot10^{-4}$	N(20%)

NO_x gradient was observed. The highest NO_x concentrations were measured in August, when the air masses arrived at Preila from the more polluted continental Europe. The same situation was observed in the year 2002. The median of NO_x concentration was 4.83 $\mu\mathrm{g/m^3}$. The concentrations of NO_x in 2000 and 2001 were lower, and for this period the air mass backward trajectories did not show any clear connection to NO_x transfer.

The highest concentrations of sulphur dioxide in Preila were measured for air masses coming from southeast, south (mostly the airborne pollutants from distant European industrial regions), and west during 1997, 2001, and 2002. The median SO_2 concentration varied between 0.93 and 3.30 $\mu\mathrm{g/m^3}$. A different situ-

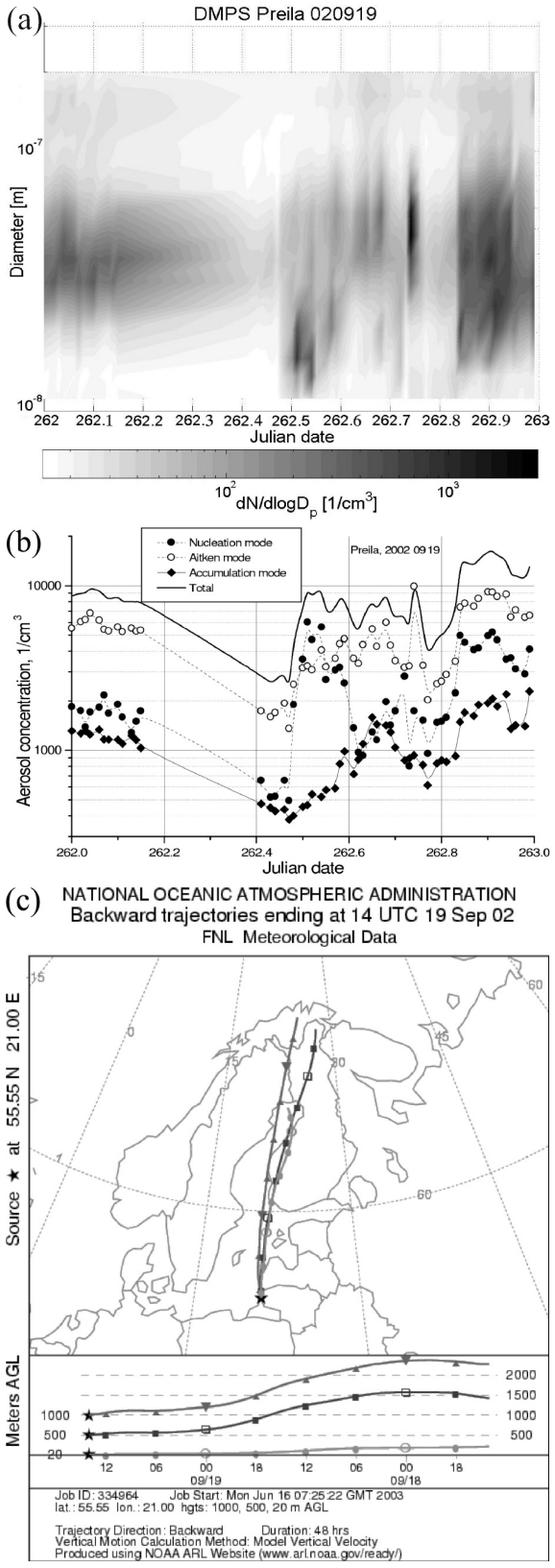

Fig. 3. (a) Time evolution of aerosol particle size distribution in Preila on 19 September 2002, (b) modal aerosol concentration, and (c) air mass backward trajectories.

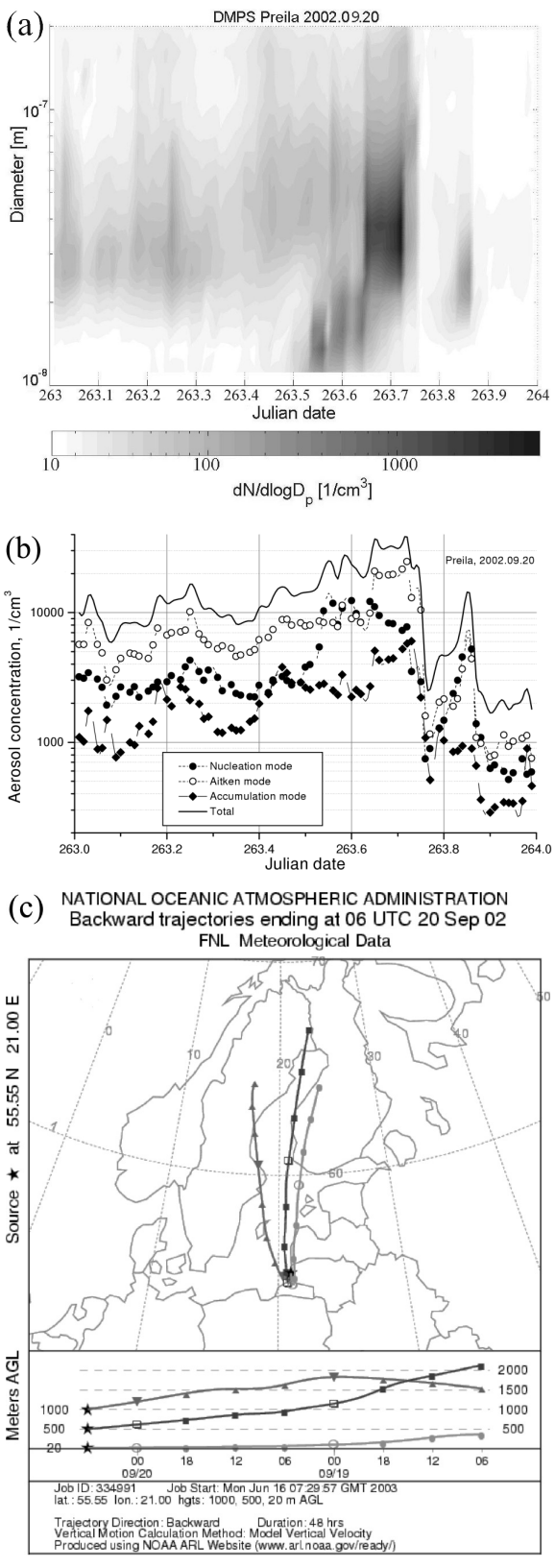

Fig. 4. (a) Time evolution of aerosol particle size distribution in Preila on 20 September 2002, (b) modal aerosol concentration, and (c) air mass backward trajectories.

ation was recorded in June 2000 when concentration of SO_2 was low: the median reached only 0.75 $\mu g/m^3$.

4.4. Aerosols

The aerosol size distributions were plotted as contour plots for each day (as a function of time). Examples of such plots, together with the number concentrations of each mode as well as air mass backward trajectories are shown in Fig. 3 for 19 September 2002 and in Fig. 4 for 20 September 2002, which were nucleation event days in Preila.

The Preila events are not as straightforward to analyse, especially in terms of growth rates, as seen in Figs. 3(a), 4(a). There is a clear formation of nucleation mode particles at the lower end of the detection limit (10 nm), but the mode does not show very clear growth (Figs. 3(b), 4(b)). Instead, the particles disappear as soon as they are formed. This disappearance might be explained by the strong mixing of air masses. However, this type of nucleation resembles the nucleation events observed in the coastal environment [19].

4.5. Nucleation and meteorological parameters

The formation of new aerosol particles appears to be highly correlated with a strong solar radiation, usually about 50–75% higher than the values recorded on non-event days. There are only a few event days when nucleation occurs at low values of solar radiation. These values are recorded when the 10 nm particles are detected in the afternoon or evening. Having in mind that the particles need some time to grow from 2–3 nm to 10 nm [20], the solar radiation was averaged for about 2–3 hours before the event time. These values are also well above the non-event day averages.

Sunny days can have a great influence on particle nucleation events because solar radiation at the same time can activate a few different independent mechanisms responsible for new particle formation. In Preila the biogenic emissions from the Baltic Sea can have influence. But these assumptions still must be investigated.

The relative humidity measured in Preila does not show any clear correlation with the particle bursts. In most of the cases, the relative humidity was higher for the event days than the average of the non-event days of the corresponding month.

Temperature and gas concentrations seem to be neutral factors for nucleation, showing no significant differences between event and non-event days. But there were some event days when SO_2 and NO_x concentrations were two or even three times higher than on non-event days. According to Boy and Kulmala [21], temperature might have an influence on nucleation during the winter when solar radiation is low, but in summer and autumn the temperature plays an insignificant role.

4.6. Characteristics of nucleation events in Preila

For each event, the growth rate is calculated graphically from the contour plots (Figs. 3(a), 4(a)), and furthermore, from the growth rate the concentration of condensable vapour can be estimated. Since the exact identity of the condensable vapour is unknown, the concentrations were estimated by using transport property values of sulphuric acid. Using the equations given in Section 3, the characteristics of nucleation event days at the Preila station were calculated. The results of those calculations are presented in Table 1.

The growth rates in Preila varied between 1.2 and 9.9 nm/h (median was 3.9 nm/h). Unusually high growth rate values were obtained for days when air masses came to the station from western directions. Therefore this can be related to higher relative humidity, which could increase the growth of nanometrical particles. The formation rate was 0.14 $cm^{-3}s^{-1}$. Such a low value of the formation rate could explain why in Preila there are so few event days when compared with other measurement stations [20, 22].

The median condensation sink was $1.5{\cdot}10^{-3}$ s^{-1}, and the vapour source rate was $8.06{\cdot}10^{4}$ $cm^{-3}s^{-1}$ in Preila. It was estimated that coagulation sinks for 1 nm particles were higher and for 3 nm particles they were lower. It means that the smaller particles exist for a shorter time because they faster coagulate with larger ambient particles. Thus, the coagulation sink can be considered as the particle characteristic lifetime.

5. Conclusions

Meteorological parameters, trace gases, and aerosol concentrations measured at Preila were analysed and characterised with respect to air masses arriving at the station. As expected, there were very distinctive diurnal trends in the measurements. Ozone, temperature, and solar radiation present a single peak at noon or soon after and can be related to the sunlight intensity. The formation of new aerosol particles is clearly related to high values of solar radiation. A low concentration of preexisting particles represents another necessary condition for nucleation to occur. The other parameters measured (temperature and gases) do not show any distinctive connection with the nucleation process.

The total aerosol concentration and size distributions were measured and analysed. For each observed nucleation event the growth rate, new particle formation rate, condensation and coagulation sinks were calculated, and the concentration of condensable vapour was estimated. The growth rates varied between 1.2 and 9.9 nm/h. The formation rate was 0.14 $\mathrm{cm}^{-3}\mathrm{s}^{-1}$. Such a low value of the formation rate could explain why in Preila there are so few event days. The median condensation sink was $1.5{\cdot}10^{-3}$ s^{-1}, and vapour source rate was $8.06{\cdot}10^{4}$ $\mathrm{cm}^{-3}\mathrm{s}^{-1}$. Preila events show a clear formation process followed by a sudden disappearance, explained, probably, by a strong mixing of air masses. This kind of nucleation appears to be characteristic of coastal environment.

However, the relatively short time of measurements in Preila does not necessarily show the annual or seasonal behaviour, and therefore further studies are required.

Acknowledgements

The research described in this paper was partially supported by the Lithuanian State Science and Studies Foundation and the FP6 Network of Excellence ACCENT. The authors are grateful for this assistance. The authors also thank Dr R. Girgždienė, Dr D. Jasinevičienė, Dr D. Šopauskienė, and Dr K. Kvietkus from the Institute of Physics for providing the data.

References

[1] M. Kulmala, H. Vehkamäki, T. Petäjä, M. Dal Maso, A. Lauri, V.-M. Kerminen, W. Birmili, and P.H. McMurry, Formation and growth rates of ultrafine atmospheric particles: A review of observations, Aerosol Science **35**, 143–176 (2004).

[2] M. Kulmala, Atmospheric science: How particles nucleate and grow, Science **302**, 1000–1001 (2003).

[3] E.D. Nilsson, J. Paatero, and M. Boy, Effects of air masses and synoptic weather on aerosol formation in the continental boundary layer, Tellus **53B**, 462–478 (2001).

[4] K.D. Perry and P.V. Hobbs, Further evidence for particle nucleation in clear air adjacent to marine cumulus clouds, J. Geophys. Res. Atmospheres **99**(D11), 22803–22818 (1994).

[5] W.A. Hoppel and G. M. Frick, Submicron aerosol size distributions measured over the tropical and South Pacific, Atmos. Env. **24A**(3), 645–660 (1990).

[6] P.M. Korhonen, M. Kulmala, A. Laaksonen, Y. Viisanen, R. McGraw, and J.H. Seinfeld, Ternary nucleation of H_2SO_4, NH_3, and H_2O in the atmosphere, J. Geophys. Res. **104**, 26349–26353 (1999).

[7] R.J. Weber, P.H. McMurry, L. Mauldin, D.J. Tanner, F.L. Eisele, F.J. Brechtel, S.M. Kreidenweis, G.L. Kok, R.D. Schillawski, and D. Baumgardner, A study of new particle formation and growth involving biogenic and trace gas species measured during ACE 1, J. Geophys. Res. **103**, 16385–16396 (1998).

[8] A.D. Clarke, D. Davis, V.N. Kapustin et al., Particle nucleation in the tropical boundary layer and its coupling to marine sulfur sources, Science **282**(5386), 89–92 (1998).

[9] M. Kulmala, L. Pirjola, and J.M. Mäkelä, Stable sulphate clusters as a source of new atmospheric particles, Nature **404**, 66–69 (2000).

[10] V. Ulevičius, G. Mordas, and K. Plauškaitė, Nucleation events at the Preila environmental research station, Environmental Chem. Phys. **24**(2), 38–44 (2002).

[11] M. Kulmala, A. Toivonen, J.M. Mäkelä, and A. Laaksonen, Analysis and growth of the nucleation mode particles observed in Boreal forest, Tellus **50B**, 449–462 (1998).

[12] M. Kulmala, *Nucleation as an Aerosol Physical Problem*, PhD thesis (University of Helsinki, Department of Physics, Helsinki, Finland, 1988).

[13] L. Pirjola, M. Kulmala, M. Wilck, A. Bischoff, F. Stratmann, and E. Otto, Effects of aerosol dynamics on the formation of the sulphuric acid aerosols and cloud condensation nuclei, J. Aerosol Sci. **30**, 1079–1094 (1999).

[14] N.A. Fuchs and A.G. Sutugin, Highly dispersed aerosol, in: *Topics in Current Aerosol Research*, eds. G.M. Hidy and J.R. Brock (Pergamon, New York, 1971).

[15] N.A. Fuchs, *The Mechanics of Aerosols* (Pergamon, London, 1964).

[16] J.H. Seinfeld and S.N. Pandis, *Atmospheric Chemistry and Physics, from Air Pollution to Climate Change* (John Wiley & Sons, New York, 1998).

[17] M.D. Allen and O.G. Raabe, Slip correction measurements of spherical solid aerosol particles in an improved Millikan apparatus, Aerosol Sci. Technol. **4**, 269–286 (1985).

[18] `http://www.arl.noaa.gov/ready.htm`

[19] C. O'Dowd, K. Hämeri, J.M. Mäkelä et al., A dedicated study of new particle formation and fate in the coastal enviroment (PARFORCE); Overview of objectives and achievements, J. Geophys. Res., **107**(D19), PAR1 (1–16) (2002).

[20] K. Plauškaitė, A. Gaman, K.E.J. Lehtinen, G. Mordas, V. Ulevičius, and M. Kulmala, A comparison study of meteorological parameters, trace gases and nucleation events in Preila and Hyytiälä, Environmental Chem. Phys. **25**(2), 60–69 (2003).

[21] M. Boy and M. Kulmala, Nucleation events in the continental boundary layer: Influence of physical and meteorological parameters, Atmos. Chem. Phys. **2**, 1–16 (2002).

[22] C.D. O'Dowd, E. Becker, and M. Kulmala, Midlatitude North-Atlantic aerosol characteristics in clean and polluted air, Atmospheric Research **58**, 167–185 (2001).

NAUJŲ DALELIŲ SUSIDARYMO IR AUGIMO PREILOS STOTYJE PARAMETRIZACIJA

K. Plauškaitė, R. Kazlauskaitė, J. Andriejauskienė, V. Ulevičius

Fizikos institutas, Vilnius, Lietuva

Santrauka

Preilos aplinkos tyrimų stotyje buvo stebimas aerozolio dalelių susidarymas ir tolesnis jų augimas aplinkos ore. Stebėti trumpi aiškaus jų susidarymo procesai, kurių eigą galima aiškinti intensyviu kai kurių parametrų kitimu. Tokio tipo nukleacija būdinga pajūrio zonoms. Kiekvienam nukleacijos epizodui buvo apskaičiuotas dalelių augimo greitis, naujų dalelių susidarymo sparta, kondensacinis ir koaguliacinis nuotėkiai, įvertinta galinčių kondensuotis garų koncentracija. Augimo greičiai kito nuo 1,2 iki 9,9 nm/h, neįprastai didelės jų vertės buvo gautos tuomet, kai oro masių pernaša buvo vakarų krypties. Tai gali būti susiję su didesne santykine drėgme, galėjusia paspartinti nanometrinių dalelių augimą. Naujų dalelių susidarymo sparta buvo 0,14 $\mathrm{cm}^{-3}\mathrm{s}^{-1}$. Tokia maža sparta gali paaiškinti, kodėl Preiloje yra mažas stebimų epizodų kiekis. Didžioji jų dalis susidarė, kai oro masių pernaša buvo iš šiaurės ar šiaurės vakarų. Kondensacinis nuotėkis buvo $1{,}3{\cdot}10^{-3}$ s^{-1}, o galinčių kondensuotis garų šaltinio sparta – $8{,}06{\cdot}10^{4}$ $\mathrm{cm}^{-3}\mathrm{s}^{-1}$. Apskaičiuota, kad koaguliaciniai nuotėkiai 1 nm dalelėms yra didesni, o 3 nm – mažesni. Tai reiškia, kad mažesnės dalelės egzistuoja trumpesnį laiką, nes greičiau koaguliuoja su kitomis aplinkoje esančiomis dalelėmis. Taigi, koaguliacinis nuotėkis gali apibūdinti dalelės gyvavimo trukmę. Vis dėlto santykinai trumpas matavimų laikas nebūtinai atspindi naujų dalelių susidarymo savybes metų sezonais, todėl yra būtini tolimesni tyrimai.